

Supporting Information

Atomic Layer Deposition of PbS Thin Films at Low Temperatures

Georgi Popov,^{†*} Goran Bačić,[‡] Miika Mattinen,[†] Toni Manner,[§] Hannu Lindström,[⊥] Heli Seppänen,[#] Sami Suihkonen,[#] Marko Vehkamäki,[†] Marianna Kemell,[†] Pasi Jalkanen,^{||} Kenichiro Mizohata,^{||} Jyrki Räisänen,^{||} Markku Leskelä,[†] Hanna Maarit Koivula,[§] Seán T. Barry,[‡] Mikko Ritala^{†*}

[†] Department of Chemistry, University of Helsinki, P.O. Box 55, FI-00014 Helsinki, Finland

[‡] Department of Chemistry, Carleton University, 1125 Colonel By Drive, Ottawa, Ontario K1S 5B6, Canada

[§] Department of Food and Nutrition, University of Helsinki, P.O. Box 66, FI-00014 Helsinki, Finland

[⊥] VTT Technical Research Centre of Finland Ltd., P.O. Box 1100, FI-90590, Oulu, Finland

[#] Department of Electronics and Nanoengineering, Aalto University, P.O. Box 13500, FI-00076, Espoo, Finland

^{||} Department of Physics, University of Helsinki, P.O. Box 43, FI-00014 Helsinki, Finland

Table of contents

Table S1. Energetics of reactions considered in the discussion of the mechanism of elemental lead formation	page S2
Table S2. Element concentrations measured with TOF-ERDA in PbS films	page S4
Table S3. Band gaps reported for PbS films in literature	page S5
Figure S1. Visual appearance of ALD PbS thin films on Si and glass	page S6
Figure S2. Influence of purge duration on the GPC of PbS films	page S6
Figure S3. PbS film thickness on sapphire	page S6
Figure S4. Uniformity of PbS films	page S7
Figure S5. Light element impurities in PbS films and depth profiles of the films	page S8
Figure S6. Influence of deposition parameters on growth of PbS _x film with Pb(dbda) at 135 °C	page S9
Figure S7. XRD patterns and photographs of PbS _x films deposited with Pb(dbda) at 135 °C	page S10
Figure S8 – S9. FESEM images of PbS films deposited at different temperatures	page S11 - 12
Figure S10. Optical properties of PbS films, transmittance and Tauc plots	page S13
Figure S11. FESEM images of PbS films deposited with different number of cycles	page S14
Figure S12. Contour profile maps of XRD data of PbS films	page S15
Figure S13. Crystallite sizes as a function of deposition temperature in PbS films	page S15
Figure S14. Optical properties of PbS films, log (1/T) and Tauc plots	page S16
Figure S15. XRD pattern of MAPI (CH ₃ NH ₃ PbI ₃) film before and after exposure to H ₂ S	page S17
Figure S16 – S17. XRD patterns of Si/MAPI/PbS film stacks at different PbS deposition temperatures	page S18 - 19
Figure S18. XRD patterns of MAPI film stored in ambient air	page S20
Figure S19. EDS line scans of Si/MAPI/PbS film stack	page S21
Figure S20-S22. XRD patterns of Si/MAPI/PbS and Si/MAPI Al ₂ O ₃ film stacks stored in ambient air	page S20 - 24
Figure S23. Oxygen and water vapor transmission of BoPET films with PbS film coating	page S25
Figure S24. Adapter for depositions on BoPET	page S25
References	page S26

Table S1. Energetics of reactions considered in the discussion of the mechanism of elemental lead formation with Pb(dbda) at higher temperatures. The energies are calculated at the temperature of 298.15 K.

Reaction	ΔH (kJ/mol)	ΔS (kJ/K mol)	ΔG (kJ/mol)
<i>PbS deposition reactions</i>			
$\text{Pb}(\text{btsa})_2 + \text{H}_2\text{S} \rightarrow \text{PbS (s)} + 2 \text{H}(\text{btsa})$	-230	0.074	-250
$\text{Pb}(\text{dbda}) + \text{H}_2\text{S} \rightarrow \text{PbS (s)} + \text{H}_2(\text{dbda})$	-300	-0.10	-270
<i>Pb(dbda) thermolysis</i>			
$\text{Pb}(\text{dbda}) \rightarrow \text{Pb} + 2 \text{N-tert-butylacetalimine}$	82	0.088	56
$\text{H}_2(\text{dbda}) \rightarrow 2 \text{N-tert-butylacetalimine} + \text{H}_2$	150	0.36	43
$\text{Pb}(\text{dbda}) + \text{H}_2(\text{dbda}) \rightarrow \text{Pb} + \text{H}_2 + 4 \text{N-tert-butylacetalimine}$	240	0.45	110
<i>Reduction by H₂S</i>			
$\text{Pb}(\text{btsa})_2 + \text{H}_2\text{S} \rightarrow \text{Pb (s)} + 2 \text{H}(\text{btsa}) + \frac{1}{8} \text{S}_8$	8.9	-0.073	31
$\text{Pb}(\text{dbda}) + \text{H}_2\text{S} \rightarrow \text{Pb (s)} + \text{H}_2(\text{dbda}) + \frac{1}{8} \text{S}_8$	-41	-0.30	48
<i>Etching by Pb precursor</i>			
$\text{Pb}(\text{btsa})_2 + \text{PbS (s)} \rightarrow 2 \text{Pb (s)} + \text{S}(\text{btsa})_2$	390	-0.32	490
$\text{Pb}(\text{dbda}) + \text{PbS (s)} \rightarrow 2 \text{Pb (s)} + \text{S}(\text{dbda})$	370	-0.32	470
<i>Etching by free ligand</i>			
$\text{PbS (s)} + 2 \text{H}(\text{btsa}) \rightarrow \text{Pb (s)} + \text{H}_2 + \text{S}(\text{btsa})_2$	410	-0.27	490
$\text{PbS (s)} + \text{H}_2(\text{dbda}) \rightarrow \text{Pb (s)} + \text{H}_2 + \text{S}(\text{dbda})$	440	-0.054	460
$\text{PbS (s)} + \text{H}_2(\text{dbda}) \rightarrow \text{Pb (s)} + \text{H}_2\text{S} + 2 \text{N-tert-butylacetalimine}$	360	0.24	290

Table continues on the next page →

Reaction	ΔH (kJ/mol)	ΔS (kJ/K mol)	ΔG (kJ/mol)
<i>Reduction by H₂</i>			
$\text{Pb}(\text{btsa})_2 + \text{H}_2 \rightarrow \text{Pb}(\text{s}) + 2 \text{H}(\text{btsa})$	-22	-0.046	-8.3
$\text{Pb}(\text{dbda}) + \text{H}_2 \rightarrow \text{Pb}(\text{s}) + \text{H}_2(\text{dbda})$	-71	-0.27	9.3
<i>Imine thiolysis and oligomerization</i>			
$\text{H}_2\text{S} + N\text{-tert-butylacetaldimine} \rightarrow \text{thioacetaldehyde} + t\text{-butylamine}$	27	0.011	24
$\text{H}_2\text{S} + N\text{-tert-butylacetaldimine} \rightarrow \frac{1}{3} \text{cis-thioacetaldehyde trimer} + 2 t\text{-butylamine}$	-68	-0.12	-32
$\text{H}_2\text{S} + N\text{-tert-butylacetaldimine} \rightarrow \frac{1}{3} \text{trans-thioacetaldehyde trimer} + 2 t\text{-butylamine}$	-66	-0.12	-30
$\text{Pb}(\text{dbda}) + 2 \text{H}_2\text{S} \rightarrow \frac{2}{3} \text{cis-thioacetaldehyde trimer} + 2 t\text{-butylamine} + \text{Pb}$	-55	-0.15	-10
$\text{Pb}(\text{dbda}) + 2 \text{H}_2\text{S} \rightarrow \frac{2}{3} \text{trans-thioacetaldehyde trimer} + 2 t\text{-butylamine} + \text{Pb}$	-50	-0.16	-2.3
<i>Miscellaneous</i>			
$\text{H}_2\text{S} \rightarrow \text{H}_2 + \frac{1}{8} \text{S}_8$	31	-0.027	39
$\text{PbS} \rightarrow \text{Pb} + \frac{1}{8} \text{S}_8$	240	-0.15	290
$\text{PbS}(\text{g}) \rightarrow \text{PbS}(\text{s})$	-230	-0.16	-180
$\text{Pb}(\text{g}) \rightarrow \text{Pb}(\text{s})$	-200	-0.11	-170

Table S2. Element concentrations measured with TOF-ERDA in PbS films deposited with Pb(btsa)₂ and Pb(dbda). The films were deposited with 1.0 s precursor pulses and purge durations. The number of deposition cycles was chosen according to Figure 1c so that the target thickness was approximately 100 nm.

	Pb(btsa)₂ – H₂S process				Pb(dbda) – H₂S process						
Dep. Temp.	65 °C	75 °C	95 °C	115 °C	45 °C	60 °C	75 °C	95 °C	115 °C	135 °C	155 °C
Pb [at. %]	50.5 ± 0.3	50.3 ± 0.3	50.3 ± 0.3	46.5 ± 0.4	45.5 ± 0.3	46.4 ± 0.3	48.0 ± 0.3	48.0 ± 0.3	59.7 ± 0.5	75.3 ± 0.5	79.8 ± 0.5
S [at. %]	47.0 ± 0.4	47.4 ± 0.5	47.1 ± 0.5	48.7 ± 0.6	51.6 ± 0.5	51.6 ± 0.5	50.5 ± 0.4	47 ± 0.5	33.5 ± 0.6	19.7 ± 0.4	16 ± 0.3
O [at. %]	1.49 ± 0.08	1.32 ± 0.08	1.32 ± 0.09	2.78 ± 0.15	1.04 ± 0.07	0.95 ± 0.06	0.8 ± 0.06	3.6 ± 0.2	4.9 ± 0.2	3.9 ± 0.2	3.5 ± 0.2
C [at. %]	0.21 ± 0.03	0.22 ± 0.04	0.27 ± 0.04	0.53 ± 0.07	0.46 ± 0.05	0.26 ± 0.04	0.26 ± 0.03	0.54 ± 0.07	0.56 ± 0.08	0.18 ± 0.04	0.23 ± 0.05
H [at. %]	0.77 ± 0.19	0.73 ± 0.20	1.00 ± 0.24	1.47 ± 0.35	1.39 ± 0.11	0.79 ± 0.12	0.48 ± 0.05	0.88 ± 0.15	1.3 ± 0.2	0.89 ± 0.12	0.51 ± 0.08
S/Pb ratio	0.93 ± 0.01	0.94 ± 0.01	0.94 ± 0.01	1.05 ± 0.02	1.13 ± 0.01	1.11 ± 0.01	1.05 ± 0.01	0.98 ± 0.01	0.56 ± 0.02	0.26 ± 0.02	0.20 ± 0.02

Table S3. Band gaps of PbS thin films reported in literature. Feature size refers either to crystallite size or to grain size depending on the method used for its determination.

Band gap (eV)	Band gap Method	Range examined (eV)	Film thicknesses (nm)	Feature size (nm)	Feature size Method	Reference
1.4 – 1.7	Tauc	0.8 – 4.5	200	-	-	Lee et al. ¹
0.9 – 1.6	Tauc	0.6 – 2.0	200	16 – 52	Scherrer	Yeon et al. ²
1.4 – 1.6	Tauc	-	-	-	-	Kaci et al. ³
0.4 – 1.5	Tauc	0.4 – 3.0	120 – 400	70 – 90	Scherrer	Sadovnikov et al. ⁴
				40 – 70	SEM	
1.7	Tauc	1.1 – 3.5	100	-	-	Kotadiya et al. ⁵
2.5 – 2.7	Tauc	1.1 – 3.1	93 - 110	60 – 217	SEM	Göde et al. ⁶
2.7	Tauc	1.0 – 3.0	750	50	SEM	Filho et al. ⁷
1.5	Tauc	1.0 – 2.0	170	100	SEM	Mohanty et al. ⁸
0.8 – 1.3	Tauc	0.6 – 1.5	250 – 400	30 – 40	Scherrer	Hone et al. ⁹
1.8	Tauc	1.4 – 2.0	-	20 – 60	SEM	Cheraghizade et al. ¹⁰
1.0 – 1.2	Tauc	0.4 – 1.4	550	7 – 30	Williamson-Hall	Veena et al. ¹¹
				400 – 600	SEM	
1.7 – 2.3	Tauc	1.0 – 3.0	600 – 1000	17 – 44	Scherrer	Abbas et al. ¹²
1.2 – 1.8	Tauc	0.4 – 2.8	150	20 – 30	Scherrer	Motlagh et al. ¹³
1.2 – 1.5	Tauc	1.0 – 2.0	-	10 – 30	Scherrer	Thangavel et al. ¹⁴
1.0 – 1.4	Tauc	1.0 – 3.5	110 – 220	-	-	Gonzalez et al. ¹⁵
0.4 – 2.8	STM	n/a	2 – 16	30 – 150	SEM	Dasgupta et al. ¹⁶

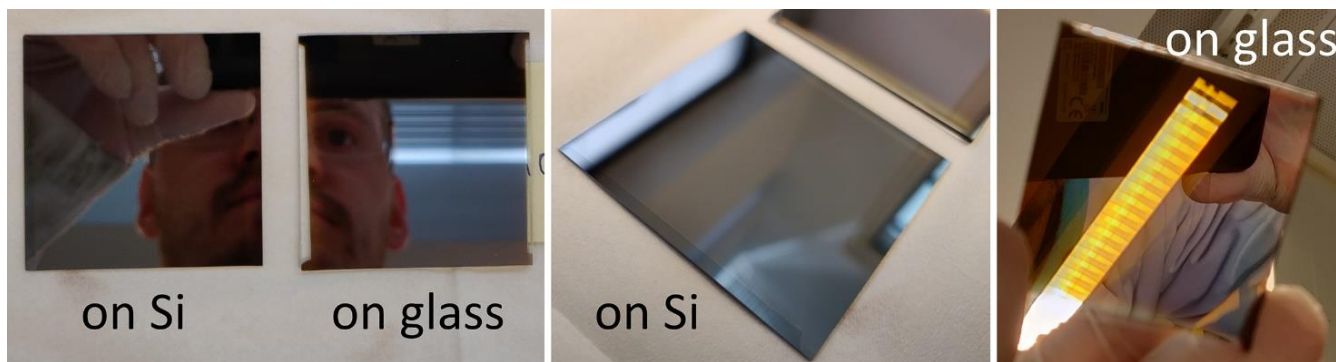


Figure S1. Photographs of PbS films deposited with $\text{Pb}(\text{btsa})_2$ and H_2S at 65°C . Precursor pulse and purge durations were 1.0 s and the number of applied deposition cycles was 1000. PbS films deposited with $\text{Pb}(\text{dbda})$ and H_2S have similar appearance. Substrate size is 5 x 5 cm.

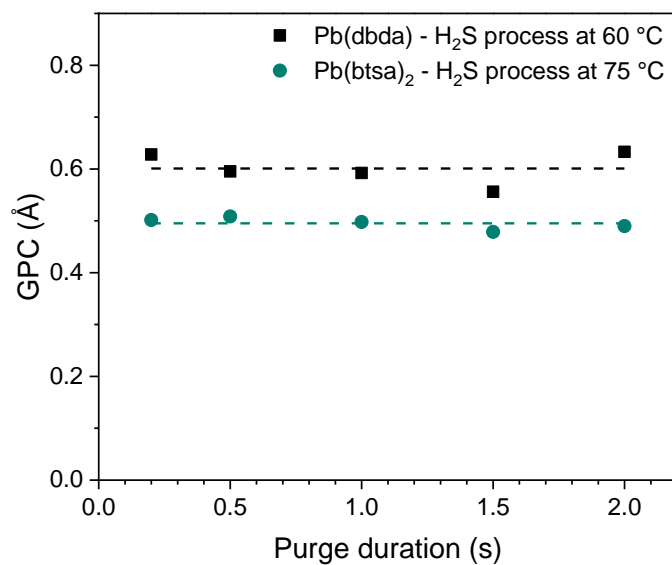


Figure S2. GPC as function of the purge duration between precursor pulses. In these experiments precursor pulse durations were fixed at 1.0 s and the number of cycles at 1000. Purge duration after both precursor pulses was varied. For example 0.5 s purge duration corresponds to a process cycle consisting of 1.0 s lead precursor pulse, 0.5 s purge, 1.0 s H_2S precursor pulse and 0.5 s purge.

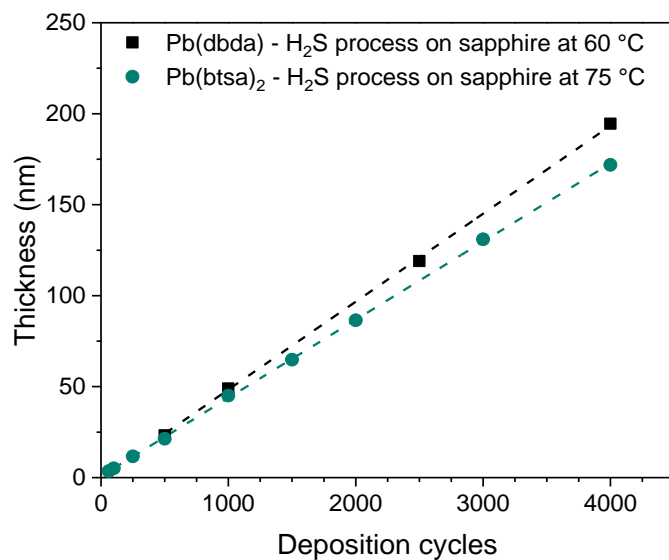


Figure S3. PbS film thickness on sapphire as a function of applied deposition cycles. Films deposited with 1.0 s precursor pulses and purge durations.

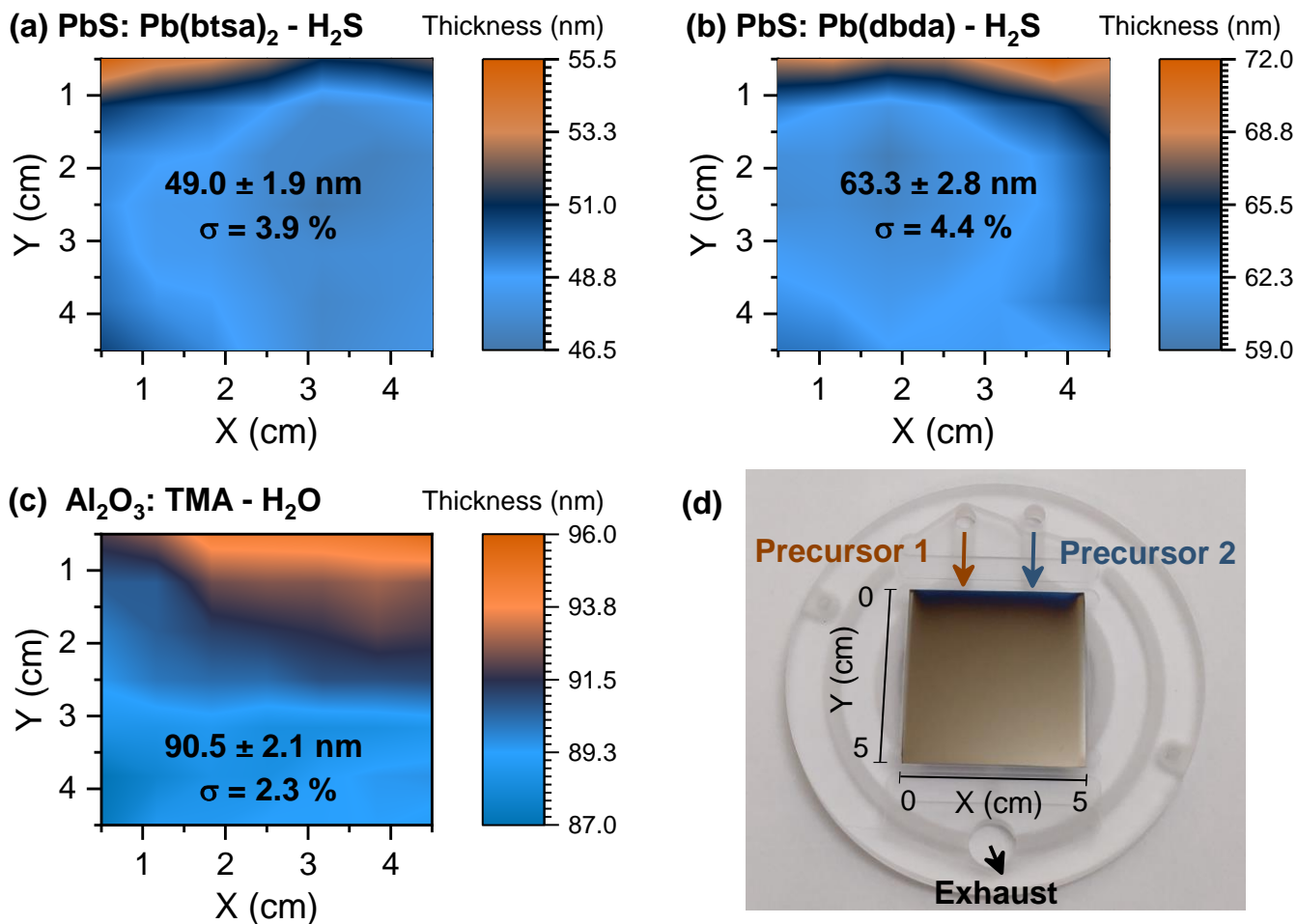


Figure S4. XRR thickness maps with 0.5 cm edge exclusion of films deposited on 5 x 5 cm² Si substrates. a) and b) are measured from PbS films deposited with 1000 cycles, 1.0 s precursor pulses and 2.0 s purge durations with Pb(btsa)₂ at 75 °C and Pb(dbda) at 60 °C respectively. c) is from a reference Al₂O₃ film deposited with trimethylaluminum (TMA) and water at 200 °C with 1000 cycles, 1.0 s precursor pulse and purge durations. In d) half of the substrate holder of the F120 ALD reactor with precursor inlets and exhaust marked with arrows is shown. If the leading edge (top 1.5 cm of the film) is excluded from the analysis, the thickness nonuniformities become 1.8 %, 2.0 % and 1.1 % for PbS made with Pb(btsa)₂, PbS made with Pb(dbda) and Al₂O₃ respectively.

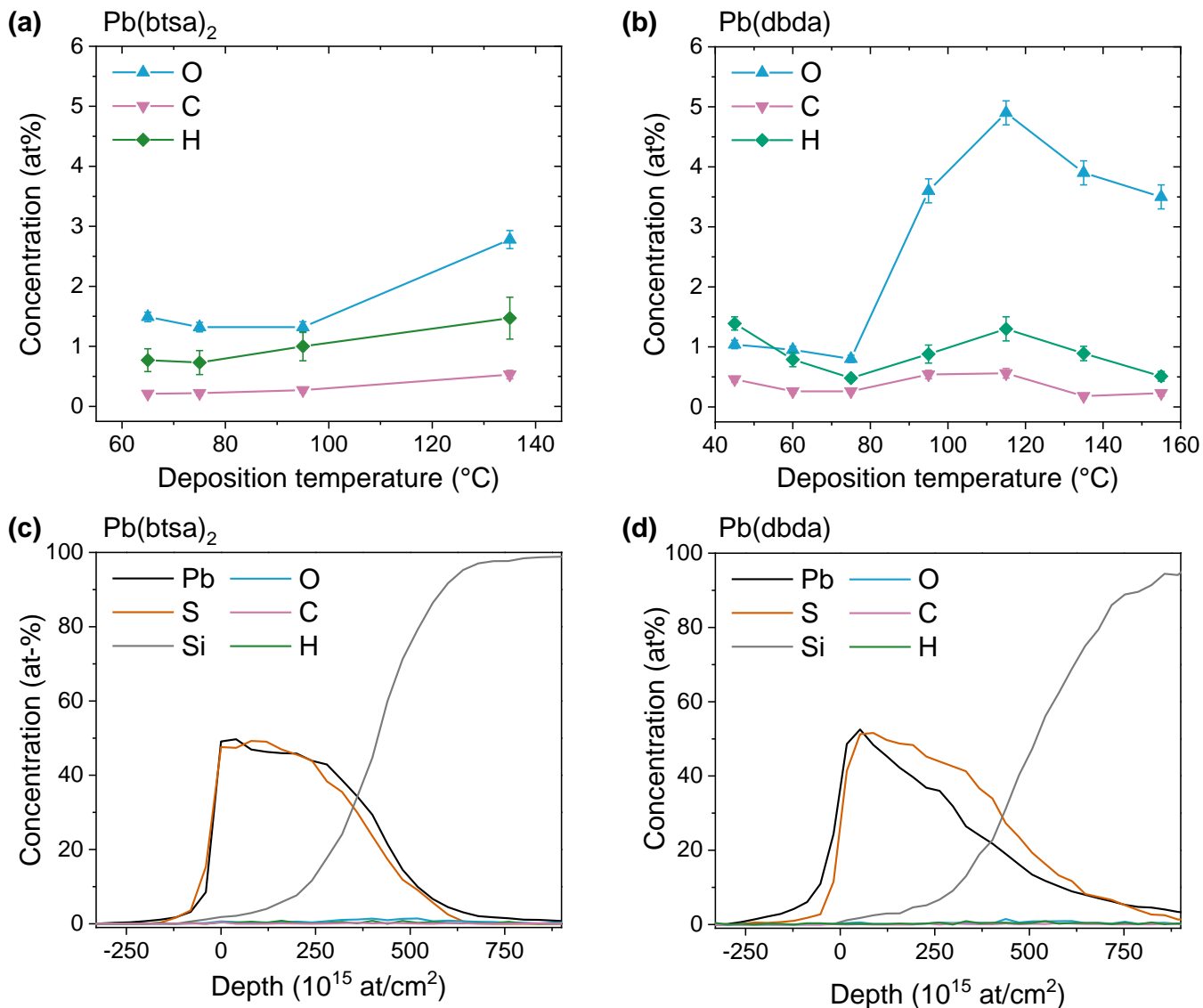


Figure S5. Impurity element concentrations measured with TOF-ERDA are shown in (a) and (b) for films made with $\text{Pb}(\text{btsa})_2$ and $\text{Pb}(\text{dbda})$ respectively. (c) and (d) show typical TOF-ERDA depth profiles. In (c) the film was deposited with $\text{Pb}(\text{btsa})_2$ at 75 $^{\circ}\text{C}$ and in (d) with $\text{Pb}(\text{dbda})$ at 60 $^{\circ}\text{C}$. The films were deposited with 1.0 s precursor pulses and purge durations. The number of deposition cycles was chosen according to Figure 1c so that the target thickness was approximately 100 nm.

Pb(dbda) at 135 °C

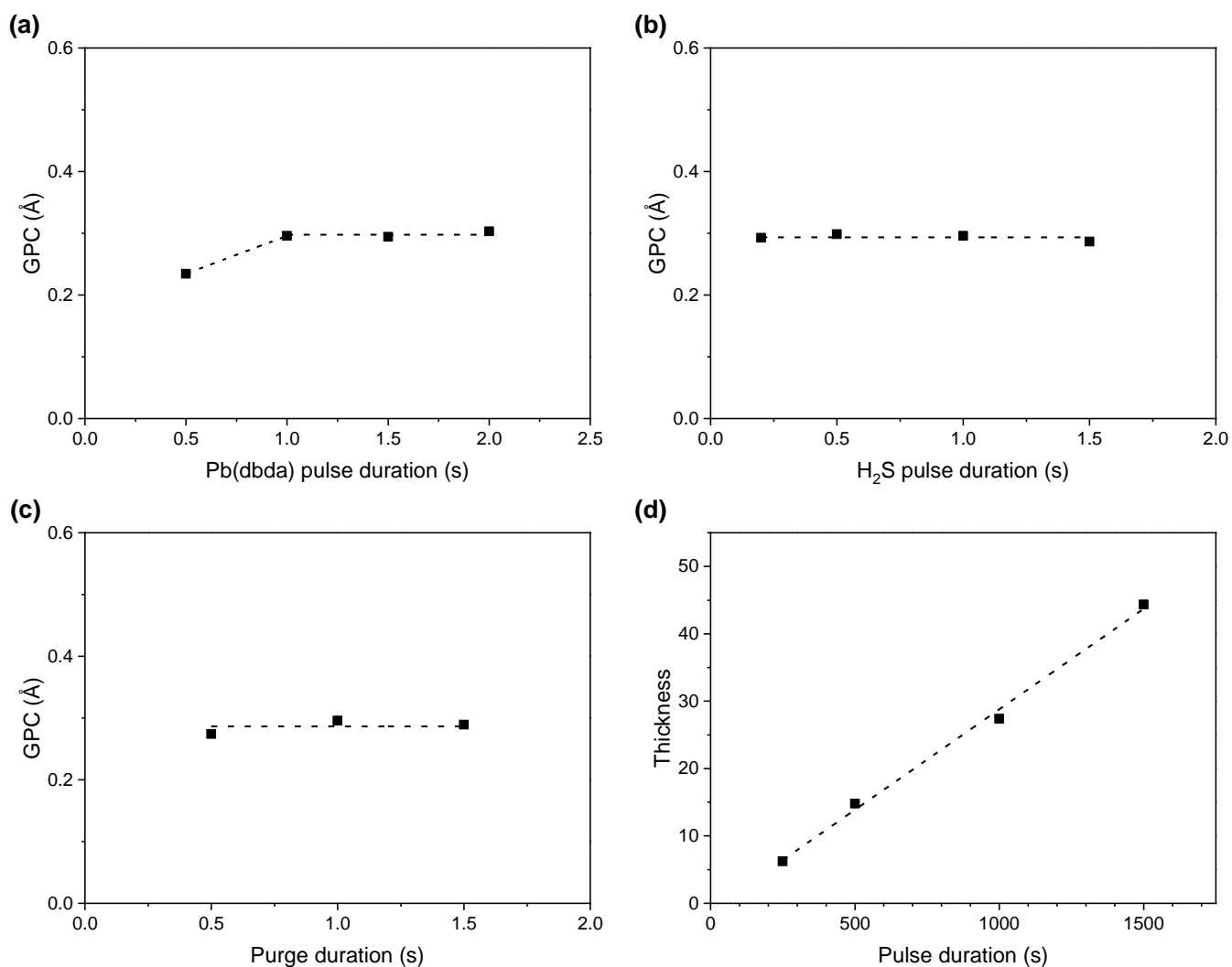


Figure S6. GPC of the PbS_x film deposited on silicon at 135 °C as a function of (a) Pb(dbda) precursor pulse duration, (b) H₂S pulse duration and (c) purge durations. (d) shows PbS_x film thickness on silicon as a function of applied deposition cycles. Unless otherwise evident, data is from films deposited with 1500 cycles, 1.0 s precursor pulses and purge durations. In (c) purge duration after both precursor pulses were varied. For example, 0.5 s purge duration corresponds to a process cycle consisting of 1.0 s lead precursor pulse, 0.5 s purge, 1.0 s H₂S precursor pulse and 0.5 s purge. In all depositions a thin underlayer (ca. 1.6 nm) and overlayer (ca. 3 nm) of Al₂O₃ was deposited prior to and after the PbS deposition. The Al₂O₃ was deposited with 1.0 s precursor pulse and 4.0 s purge durations. 25 and 50 cycles were used for the underlayer and overlayer respectively.

Pb(dbda) at 135 °C

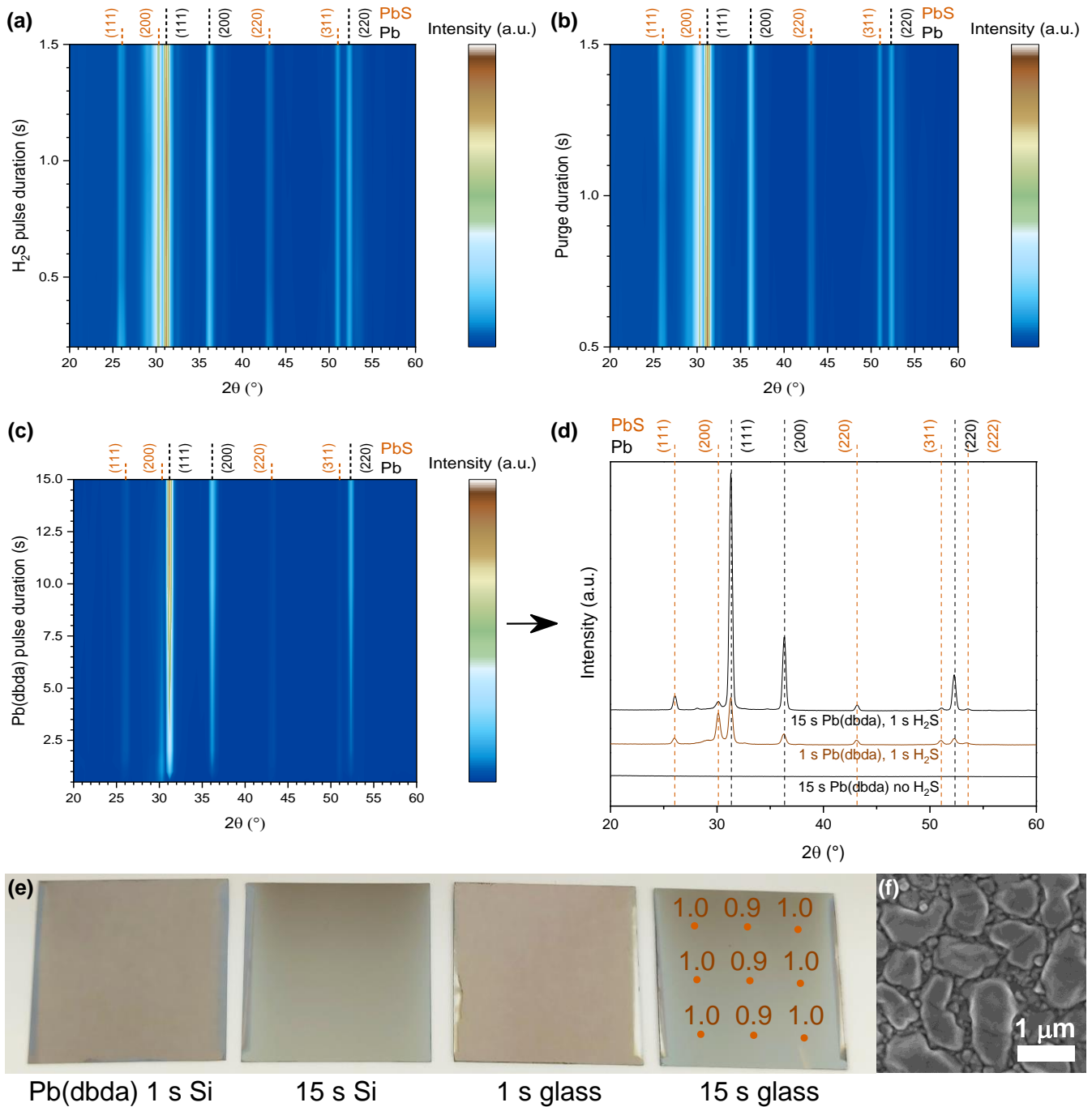


Figure S7. Contour profile maps of grazing incidence XRD (GIXRD) data for PbS_x films deposited on silicon at 135 °C as a function of (a) H₂S pulse duration, (b) purge durations and (c) Pb(dbda) precursor pulse duration. (d) shows GIXRD of films deposited with 15 s and 1 s Pb(dbda) pulse durations as well as a reference where only Pb(dbda) was pulsed for 15 s separated by 1.0 s purges. (e) Photographs of PbS_x films deposited on Si and soda lime glass with 1.0 s and 15 s Pb(dbda) pulse durations. Vermillion dots and numbers are resistivities in mΩ cm measured at that site. (f) FESEM image of a PbS_x film deposited with 15 s long Pb(dbda) pulse durations. Unless otherwise evident, data is from films deposited with 1500 cycles, 1.0 s precursor pulses and purge durations. In (b) purge durations after both precursor pulses were varied. For example, 0.5 s purge duration corresponds to a process cycle consisting of 1.0 s lead precursor pulse, 0.5 s purge, 1.0 s H₂S precursor pulse and 0.5 s purge. In all depositions a thin underlayer (ca. 1.6 nm) and overlayer (ca. 3 nm) of Al₂O₃ was deposited prior to and after the PbS deposition. The Al₂O₃ was deposited with 1.0 s precursor pulse and 4.0 s purge durations. 25 and 50 cycles were used for the underlayer and overlayer respectively.

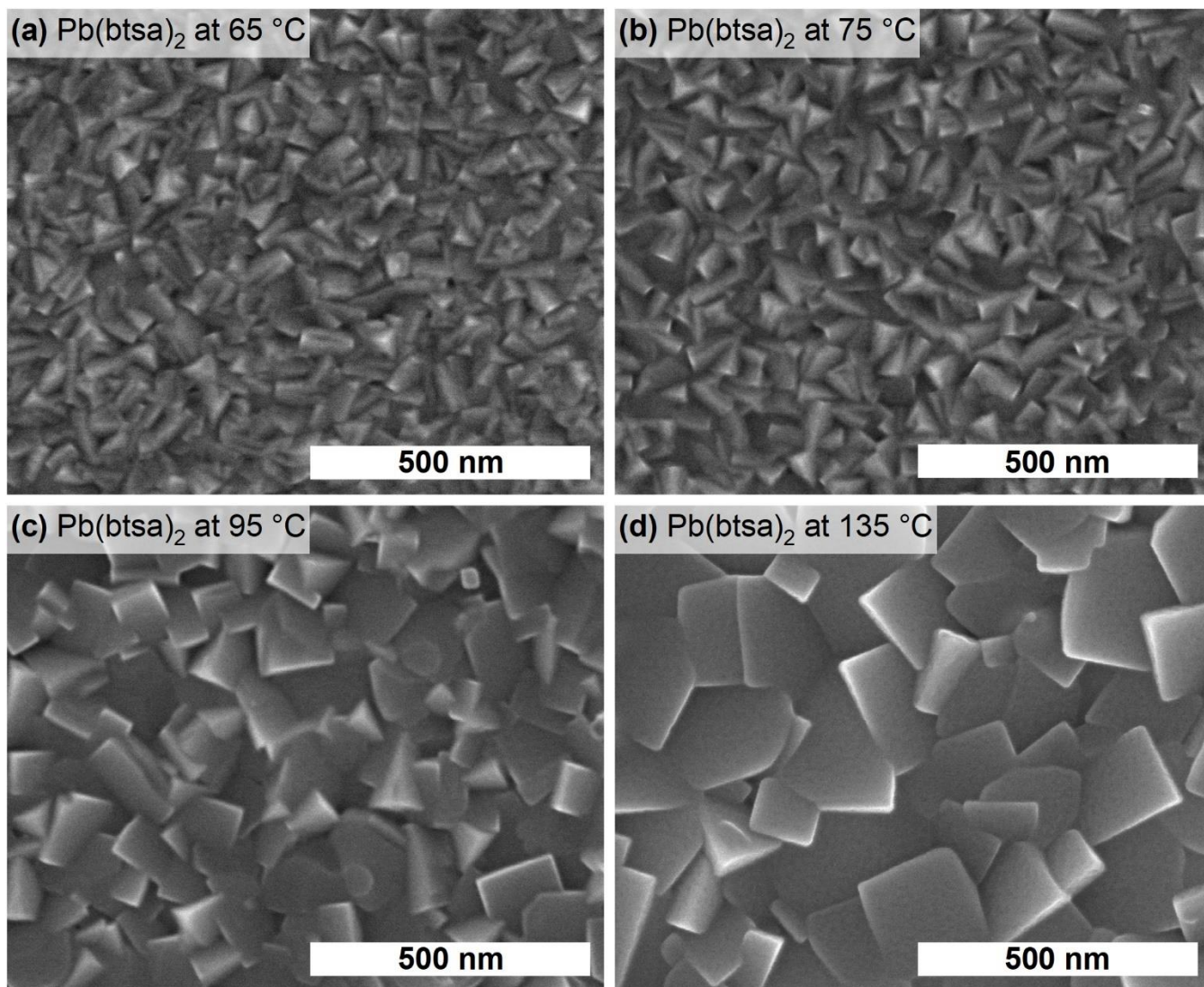


Figure S8. FESEM images of PbS films deposited at different temperatures with the $\text{Pb}(\text{btsa})_2 - \text{H}_2\text{S}$ process using 1.0 s precursor pulses and purge durations. The number of deposition cycles was chosen according to Figure 1c so that the target thickness was approximately 100 nm.

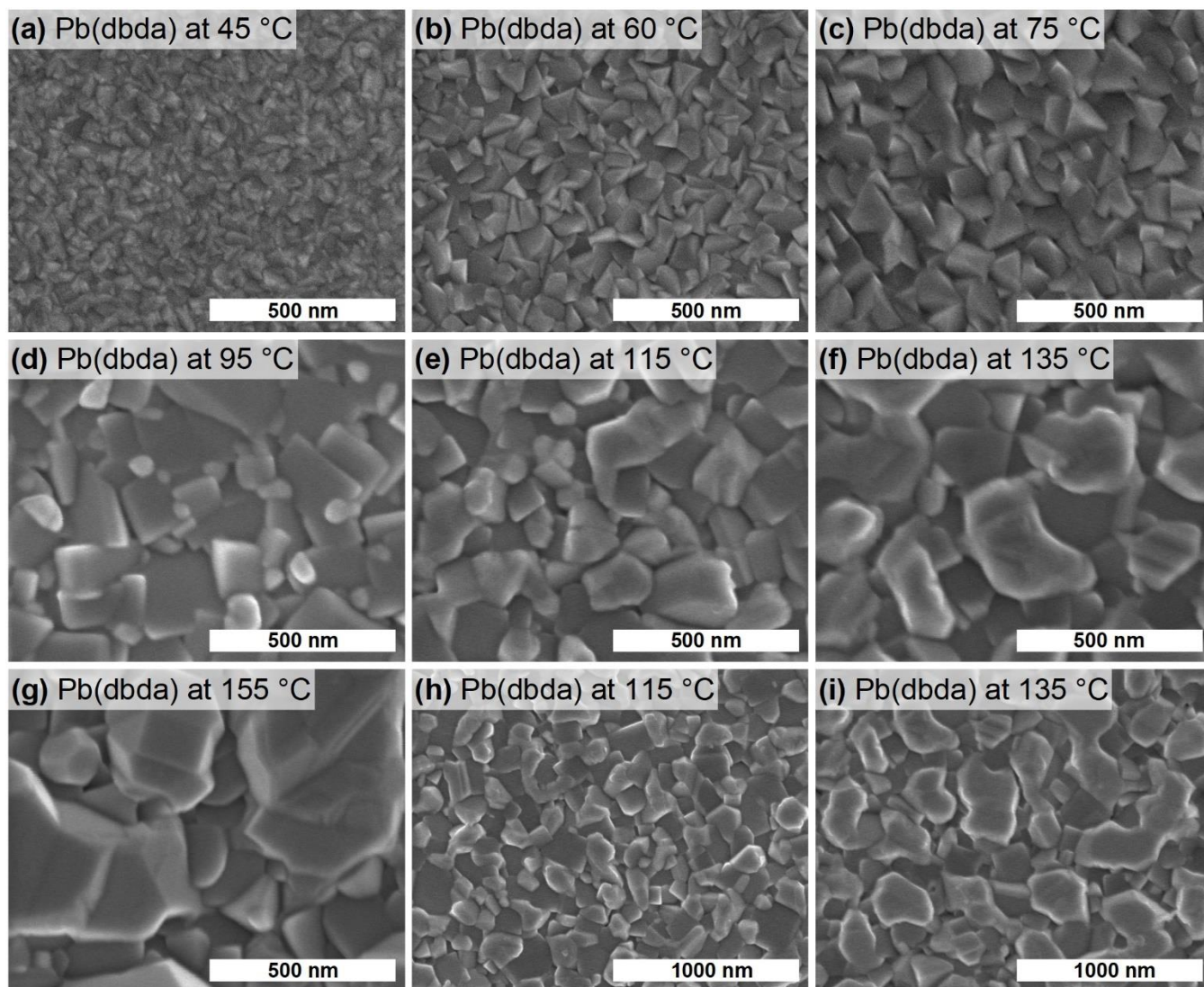


Figure S9. FESEM images of PbS films deposited at different temperatures with the Pb(dbda) – H₂S process using 1.0 s precursor pulses and purge durations. The number of deposition cycles was chosen according to Figure 1c so that the target thickness was approximately 100 nm. Note different magnifications in (h) and (i).

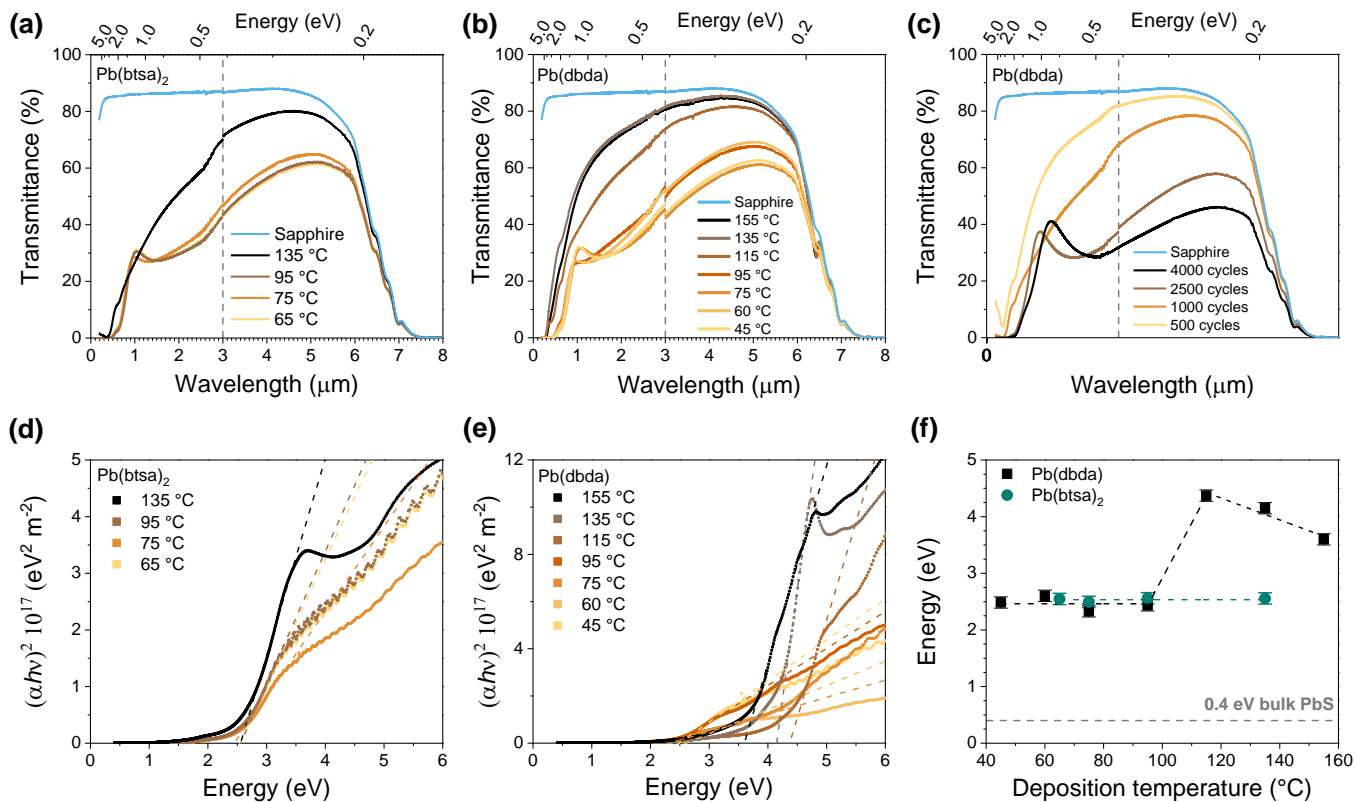


Figure S10. Transmittance of ca. 100 nm thick PbS films deposited on sapphire with (a) Pb(btsa)₂ and (b) Pb(dbda) at different temperatures. (c) Transmittance of PbS films deposited on sapphire with Pb(dbda) at 60 °C and different number of deposition cycles. (d) and (e) Tauc plots constructed from (a) and (b) respectively. (c) Optical band gaps of PbS films on sapphire as a function of deposition temperature extracted from Tauc plots in (d) and (b). Dashed grey lines in (a-c) separate wavelength ranges measured with different instruments. All films were deposited with 1.0 s precursor pulses and purge durations.

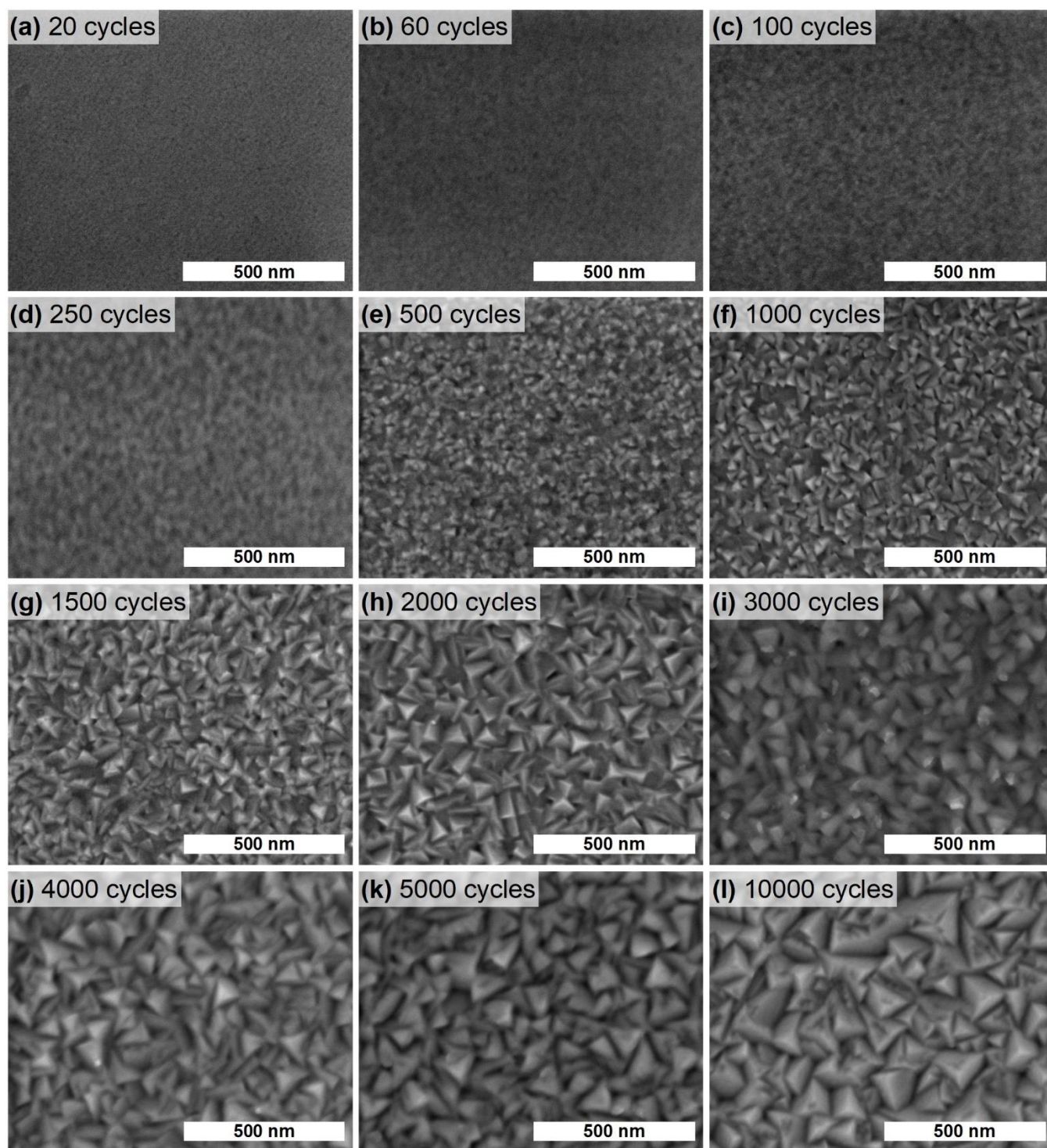


Figure S11. FESEM images of PbS films deposited with different number of cycles. The films were deposited at 75 °C with the Pb(bt₂a)₂ – H₂S process using 1.0 s precursor pulses and purge durations.

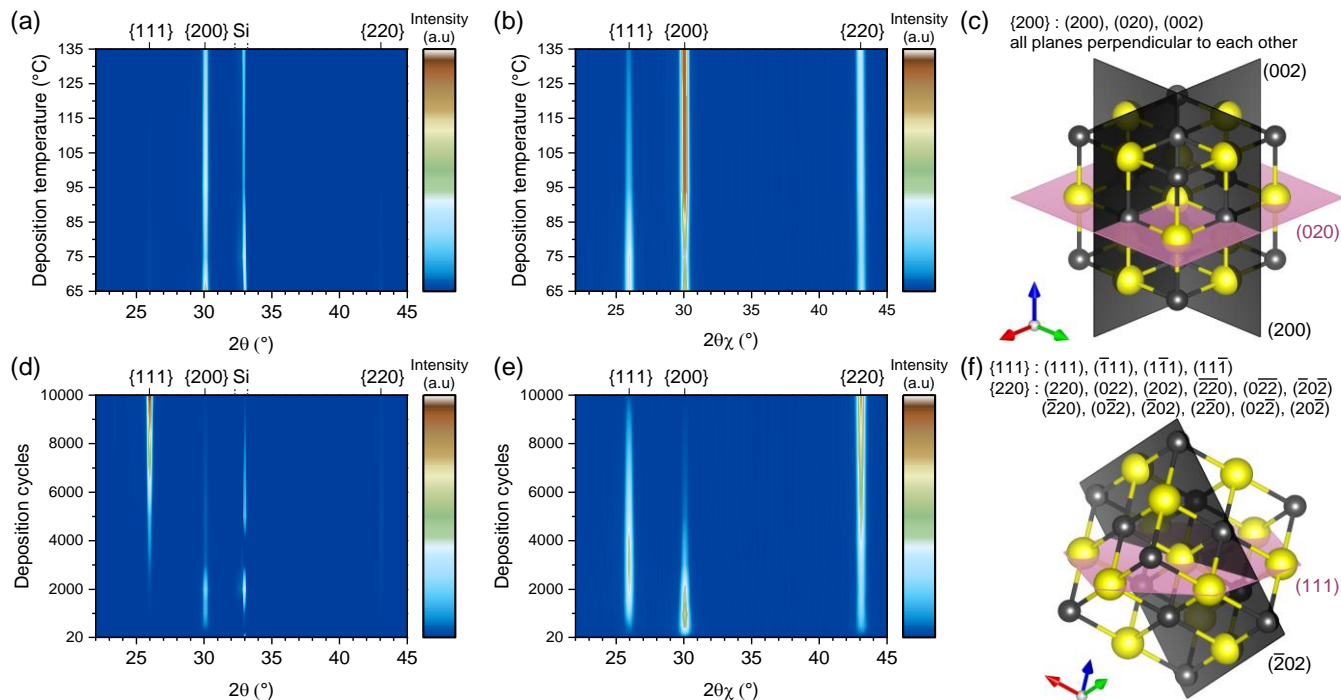


Figure S12. Contour profile maps of out of plane (a, d) and in-plane (b, e) XRD data for PbS films deposited with Pb(btsa)₂. In (a) and (b) films are ca. 100 nm thick. In (d) and (e) films were deposited at 75 °C. All films were deposited with 1.0 s precursor pulses and purge durations. (c) and (f) show the unit cell of PbS (lead is black, sulfur is yellow), list equivalent lattice planes for a cubic unit cell that belong to the {200}, {111}, {220} families and show an example of a pair of perpendicular lattice planes that can be observed in the out of plane and in-plane measurements. Note that for {111} and {220} families only the following planes are perpendicular: (111) ⊥ ($\bar{2}20$), (0 $\bar{2}2$), ($\bar{2}02$), ($\bar{2}20$), (02 $\bar{2}$), (20 $\bar{2}$); ($\bar{1}\bar{1}1$) ⊥ (220), (022), ($\bar{2}20$), ($\bar{2}02$), (0 $\bar{2}2$), (02 $\bar{2}$); ($1\bar{1}\bar{1}$) ⊥ (220), (022), ($\bar{2}20$), (0 $\bar{2}2$), ($\bar{2}02$), (20 $\bar{2}$); ($11\bar{1}$) ⊥ (022), (202), (0 $\bar{2}2$), ($\bar{2}02$), ($\bar{2}20$), ($\bar{2}20$).

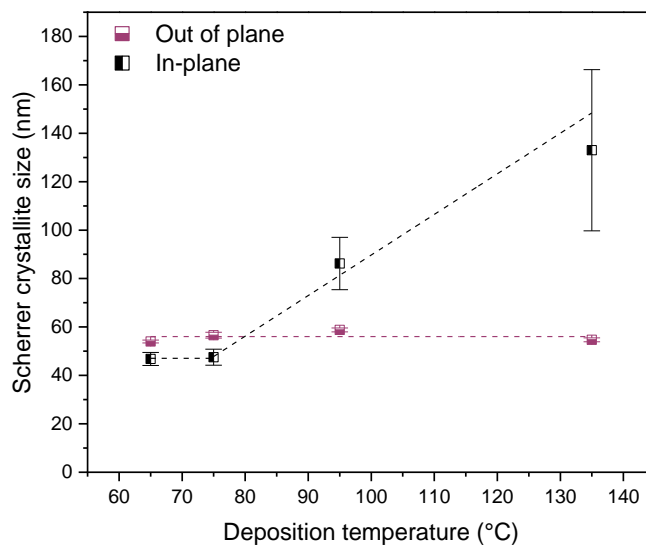


Figure S13. Out of plane and in-plane crystallite sizes in ca. 100 nm thick PbS films deposited with Pb(btsa)₂. All films were deposited with 1.0 s pulse and purge durations.

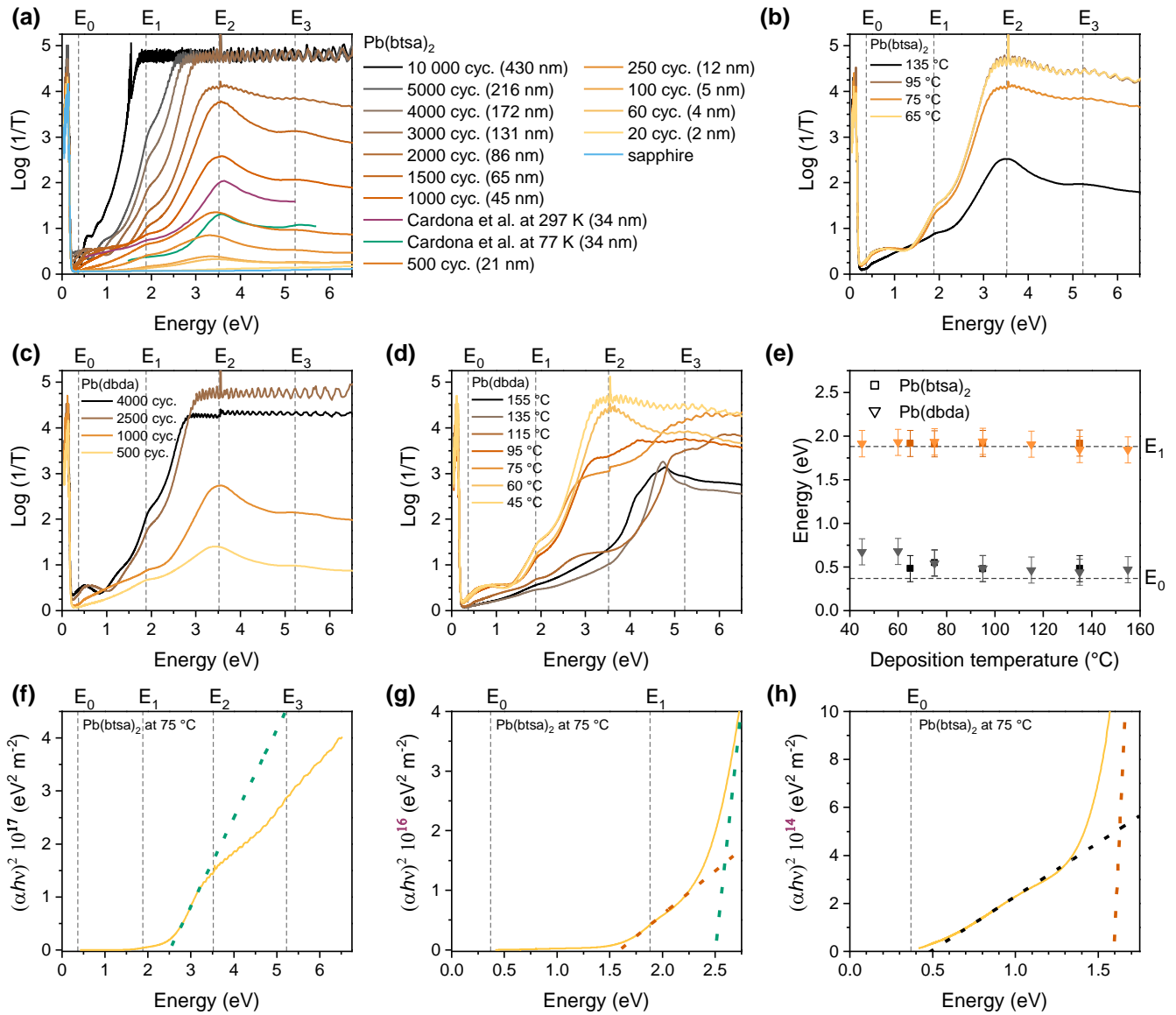


Figure S14. (a) Log (1/T) plots of PbS films deposited on sapphire with Pb(btsa)₂ at 75 °C and different number of cycles. (b) Log (1/T) plots of ca. 100 nm thick PbS films deposited on sapphire with Pb(btsa)₂ at different temperatures. (c) Log (1/T) plots of PbS films deposited on sapphire with Pb(dbda) at 60 °C and different number of cycles. (d) Log (1/T) plots of ca. 100 nm thick PbS films deposited on sapphire with Pb(dbda) at different temperatures. (e) Interband transitions energies obtained from Log (1/T) plots in (b) and (d) as a function of deposition temperature. (f-h) Tauc plot of ca. 100 nm PbS film deposited on sapphire with Pb(btsa)₂ at 75 °C. Note that changing the examined energy range and Tauc property scale ((αhv)², y-axis) allows fitting three different energies ca. 0.5 eV, 1.6 and 2.5 eV which correspond to E₀, E₁ and E₂ transitions respectively. In the analogous log (1/T) plot, see for example (b), features corresponding to these transitions are immediately visible without extensive rescaling. In all figures dashed gray lines are reference energy values by Cardona et al.¹⁷ All films were deposited with 1.0 s pulse and purge durations.

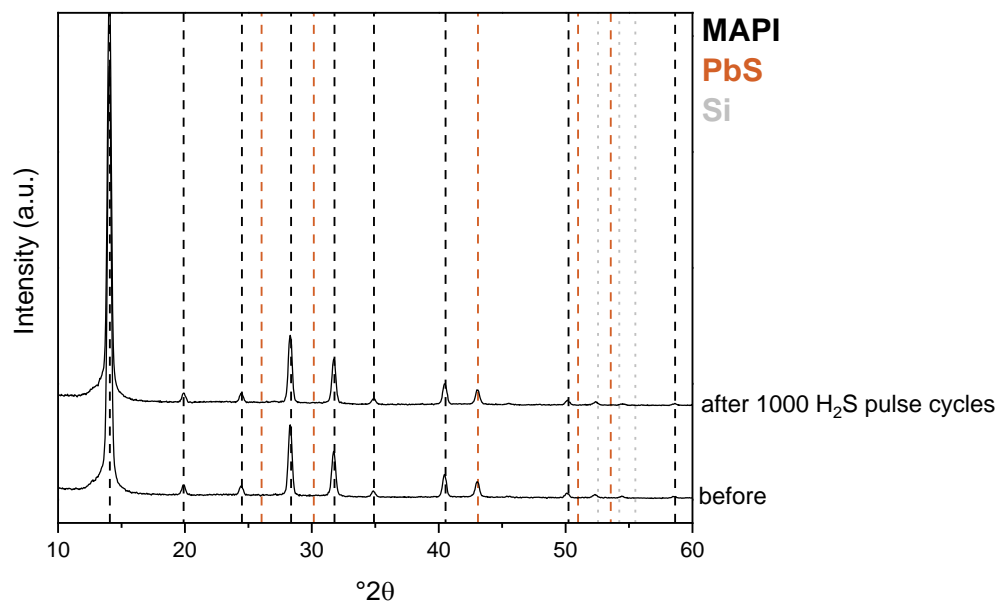


Figure S15. GIXRD pattern of a MAPI ($\text{CH}_3\text{NH}_3\text{PbI}_3$) film before and after 1000 cycles of 1.0 s long H_2S pulses separated by 3.0 s long purges at 50 °C.

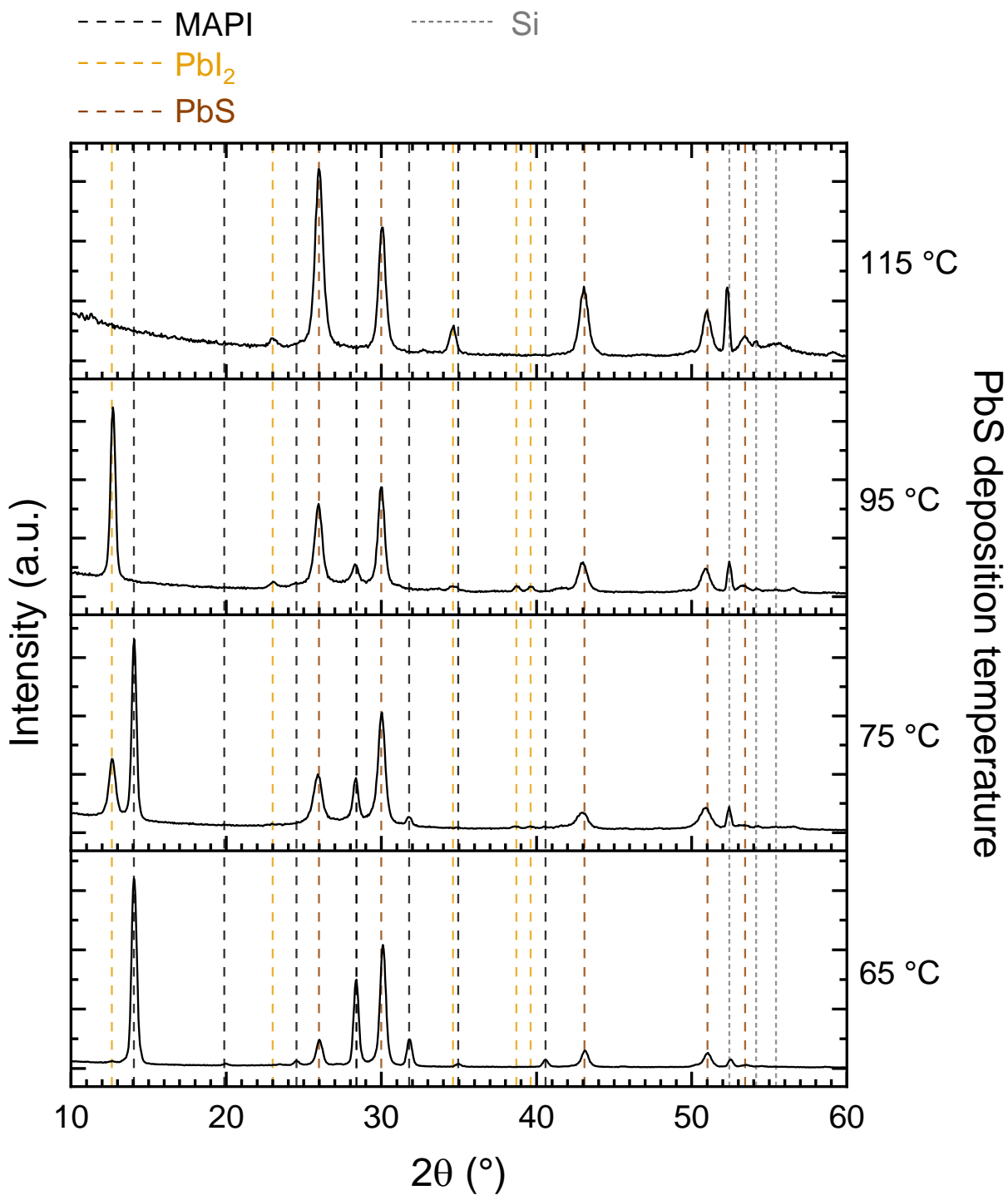


Figure S16. GIXRD patterns of samples where PbS was deposited with Pb(btsa)₂ at different temperatures on MAPI films on silicon substrates. PbS was deposited with 1000 cycles, 1.0 s precursor pulses and purge durations.

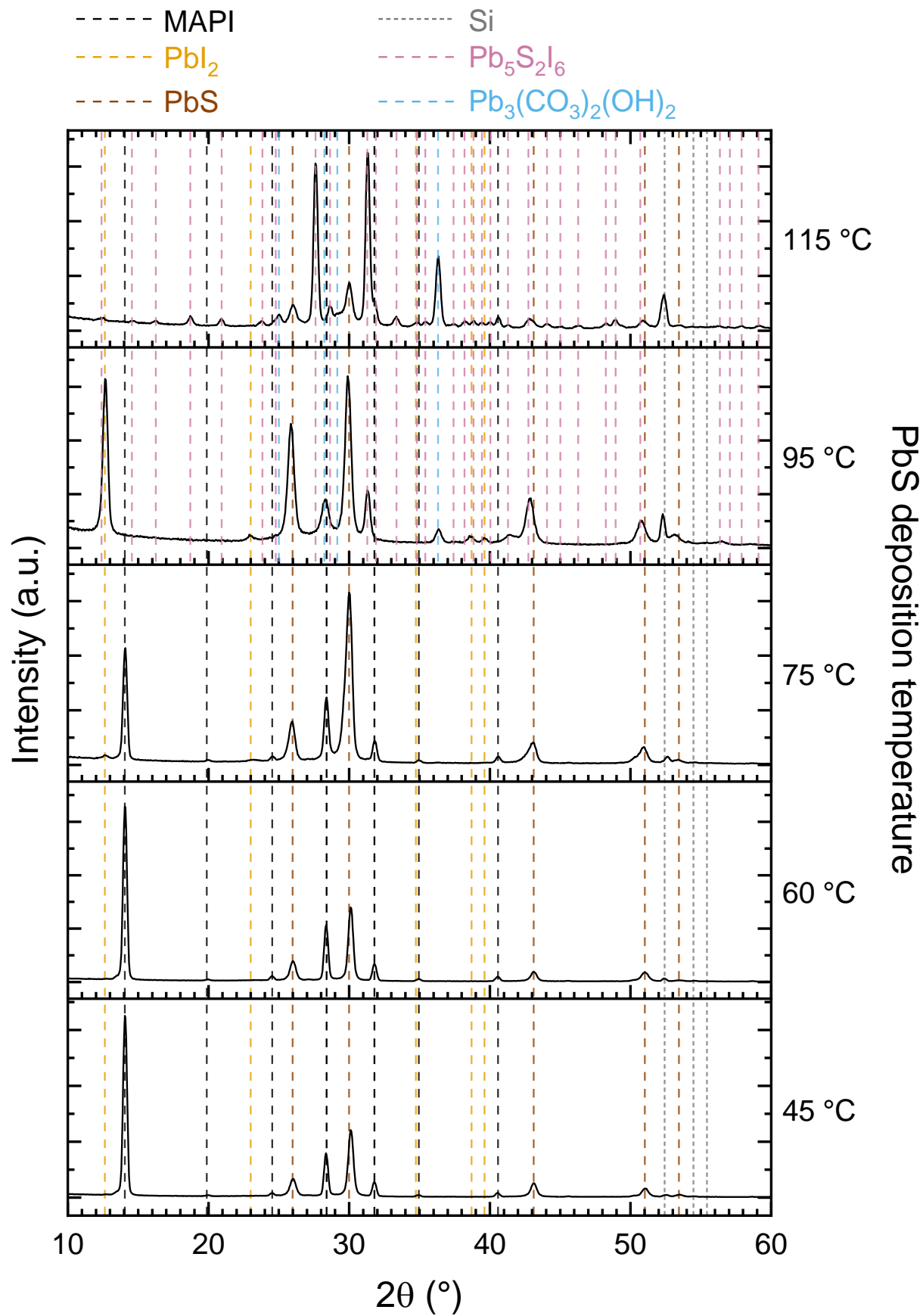


Figure S17. GIXRD patterns of samples where PbS was deposited with Pb(dbda) at different temperatures on MAPI (CH₃NH₃PbI₃) films on silicon substrates. PbS was deposited with 1000 cycles, 1.0 s precursor pulses and purge durations.

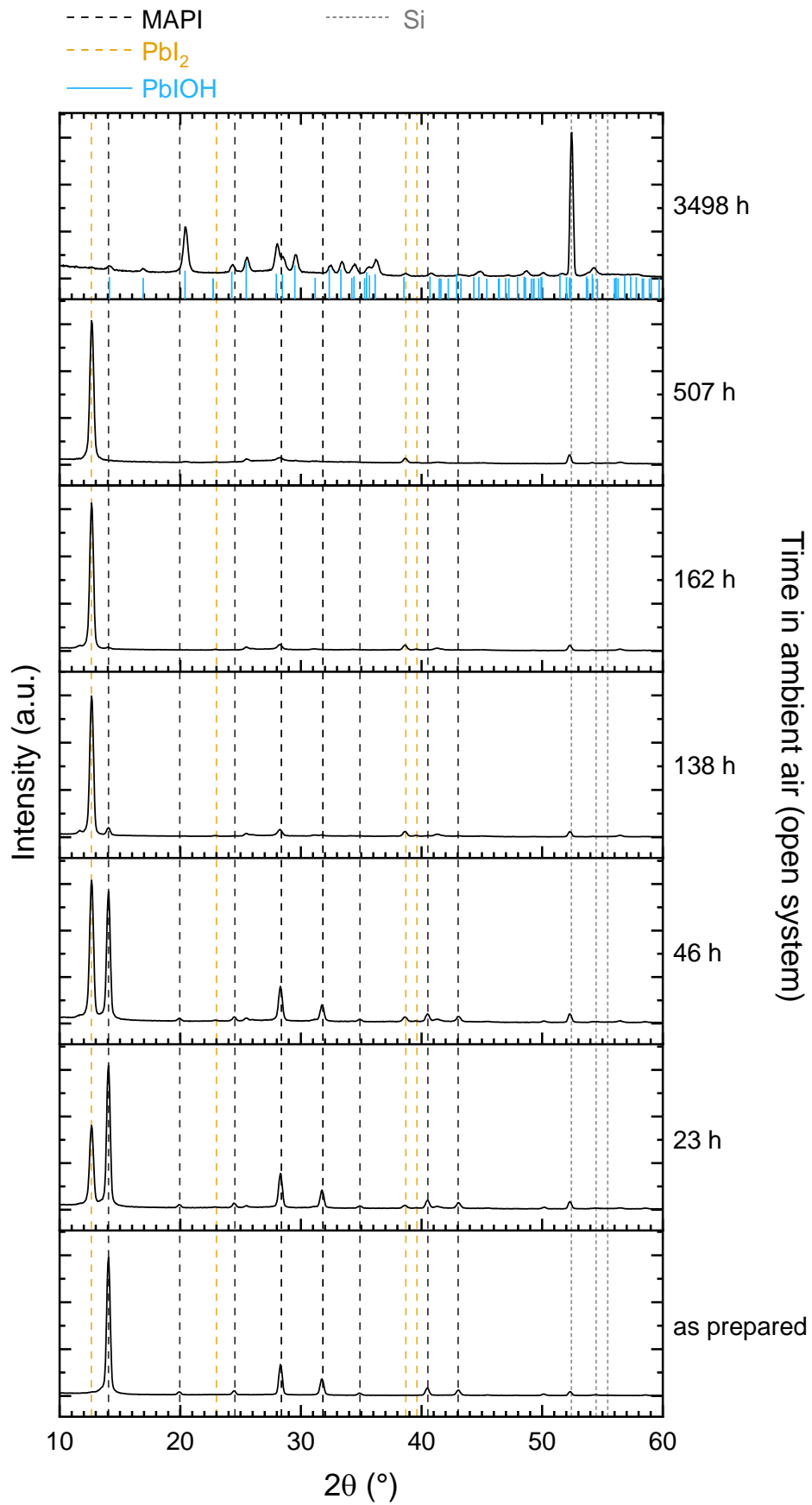


Figure S18. GIXRD patterns of MAPI film stored in ambient air.

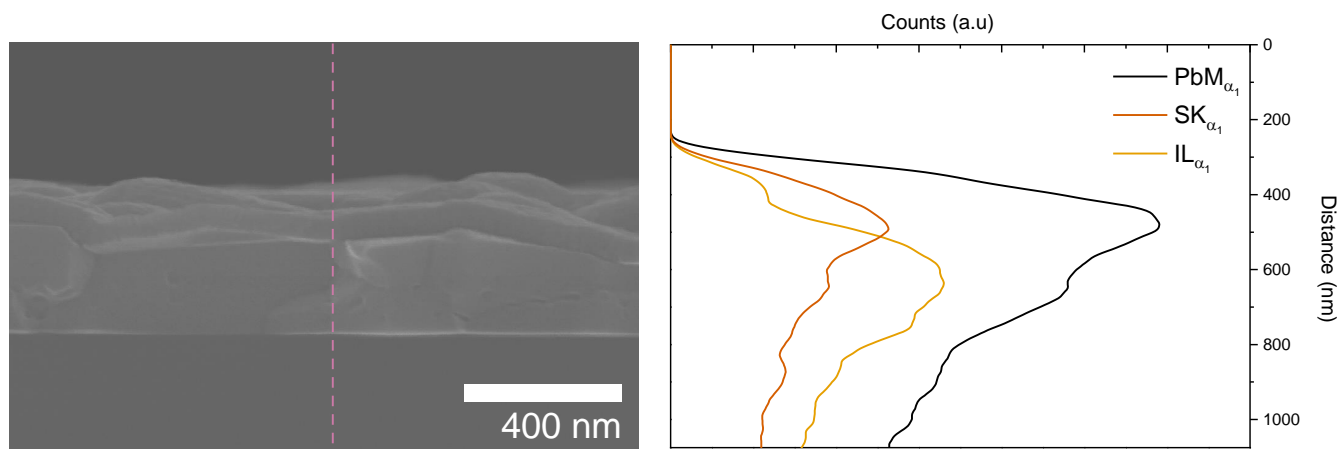


Figure S19. Cross-section SEM image of a PbS capped MAPI and EDS line scans along the purple line. PbS was deposited with Pb(dbda) at 45 °C with 1000 cycles of 1.0 s long pulse and purge durations. To examine the cross section the sample was broken in half after being stored in air for 413 days. The EDS line scan data was smoothed (adjacent averaging) for clarity. Note also the partial overlap between PbM_α and SK_α lines.

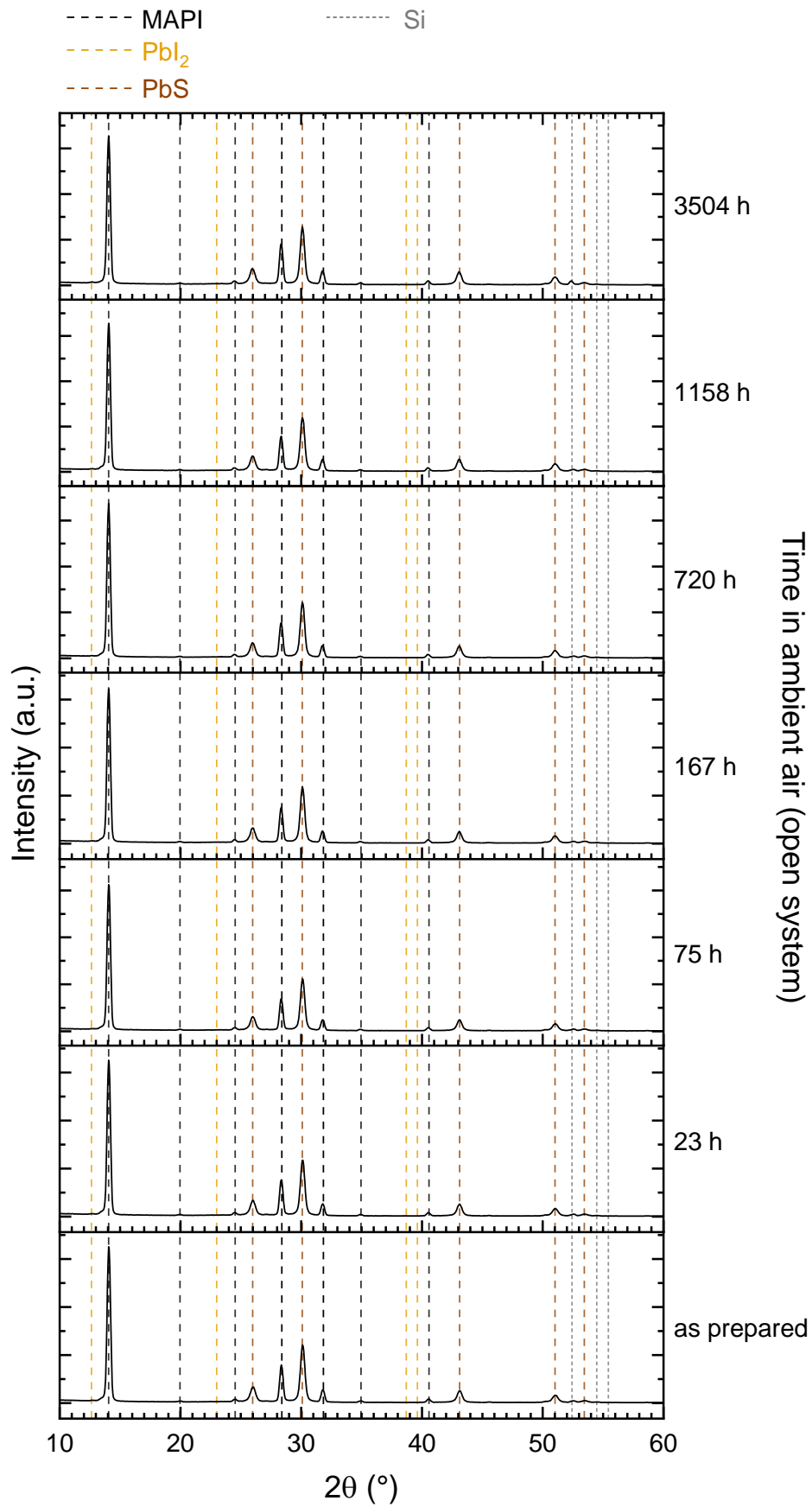


Figure S20. GIXRD patterns of a MAPI film capped with a PbS film and stored in ambient air. PbS was deposited with Pb(dbda) at 45 °C with 1000 cycles and 1.0 s precursor pulses and purge durations. The capping film thickness estimated from GPC on Si is 66 nm.

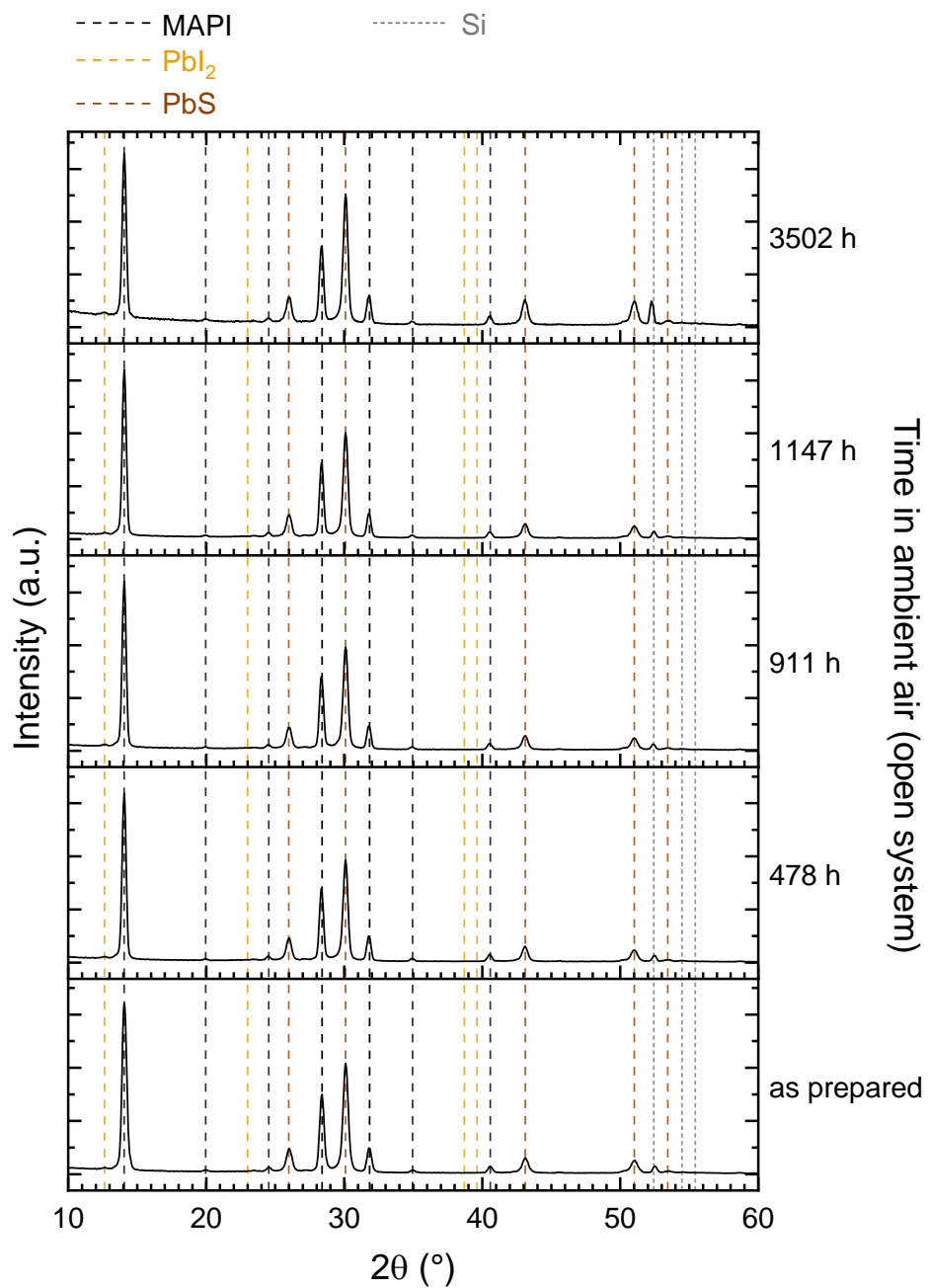


Figure S21. GIXRD patterns of a MAPI film capped with a PbS film and stored in ambient air. PbS was deposited with $\text{Pb}(\text{btsa})_2$ at 65 °C with 1000 cycles and 1.0 s precursor pulses and purge durations. The capping film thickness estimated from GPC on Si is 50 nm.

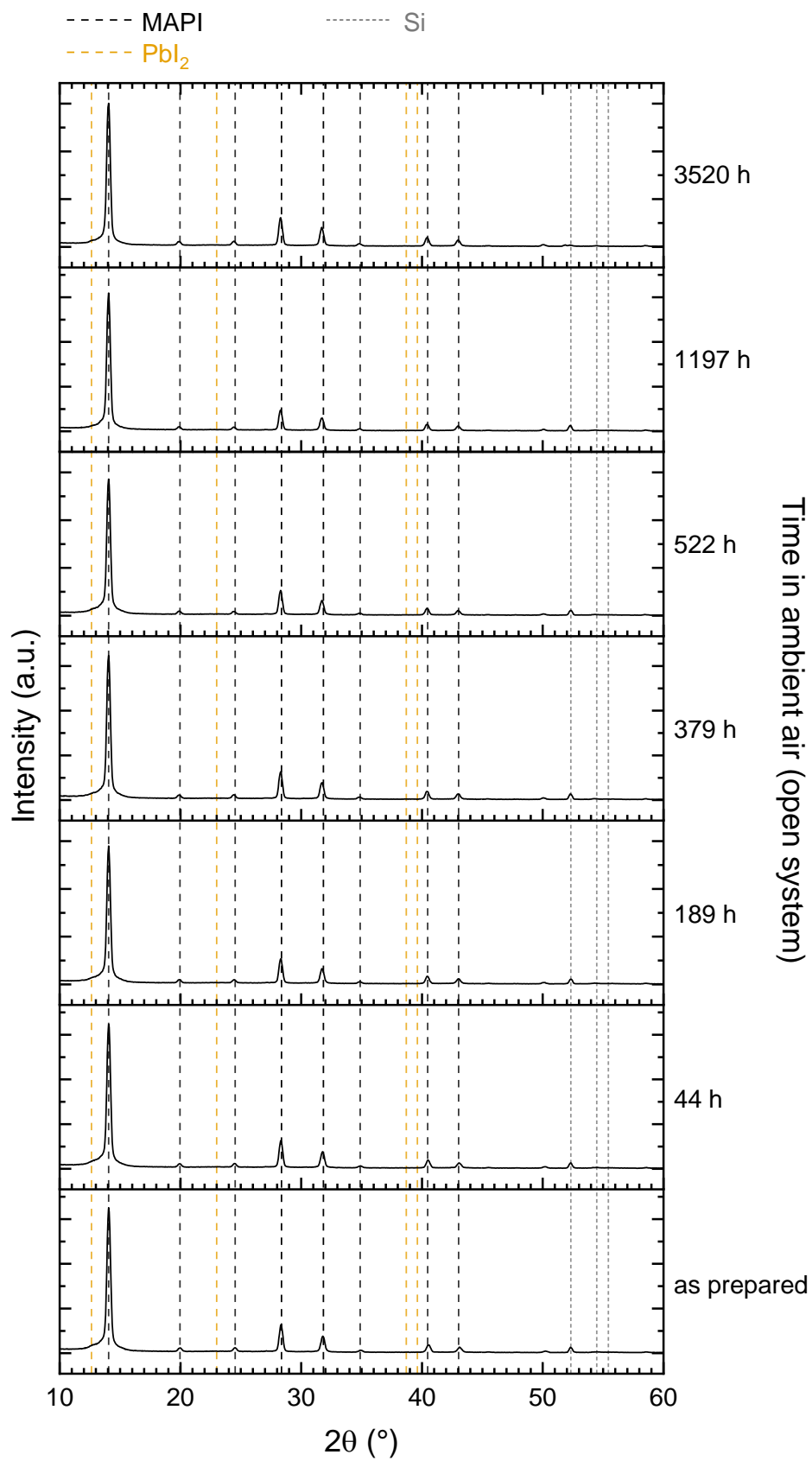


Figure S22. GIXRD patterns of a MAPI film capped with an Al₂O₃ film and stored in ambient air. Al₂O₃ was deposited with the TMA - H₂O process at 65 °C with 800 cycles, 1.0 s precursor pulses and 4.0 s purge durations. The capping film thickness estimated from GPC on Si is 52 nm.

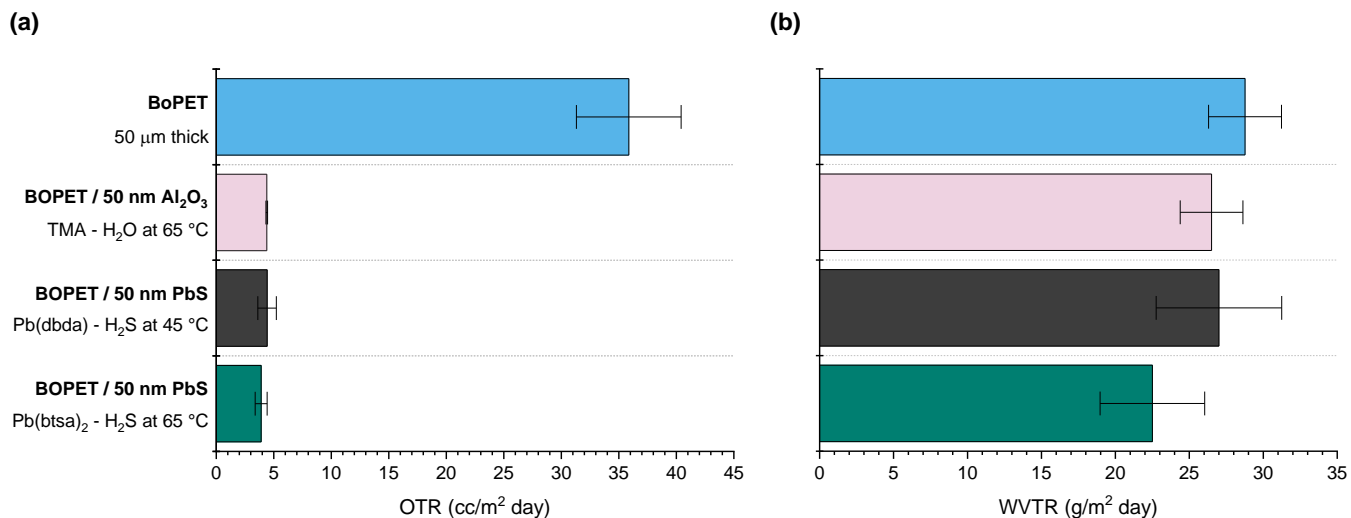


Figure S23. (a) Oxygen transmission rates and (b) water vapor transmission rates for bare BoPET and BoPET with an ALD film deposited on it. Al₂O₃ films were deposited with 1.0 s precursor pulses and 4.0 s purge durations. PbS films were deposited with 6.0 s precursor pulses and 3.0 s purge durations.

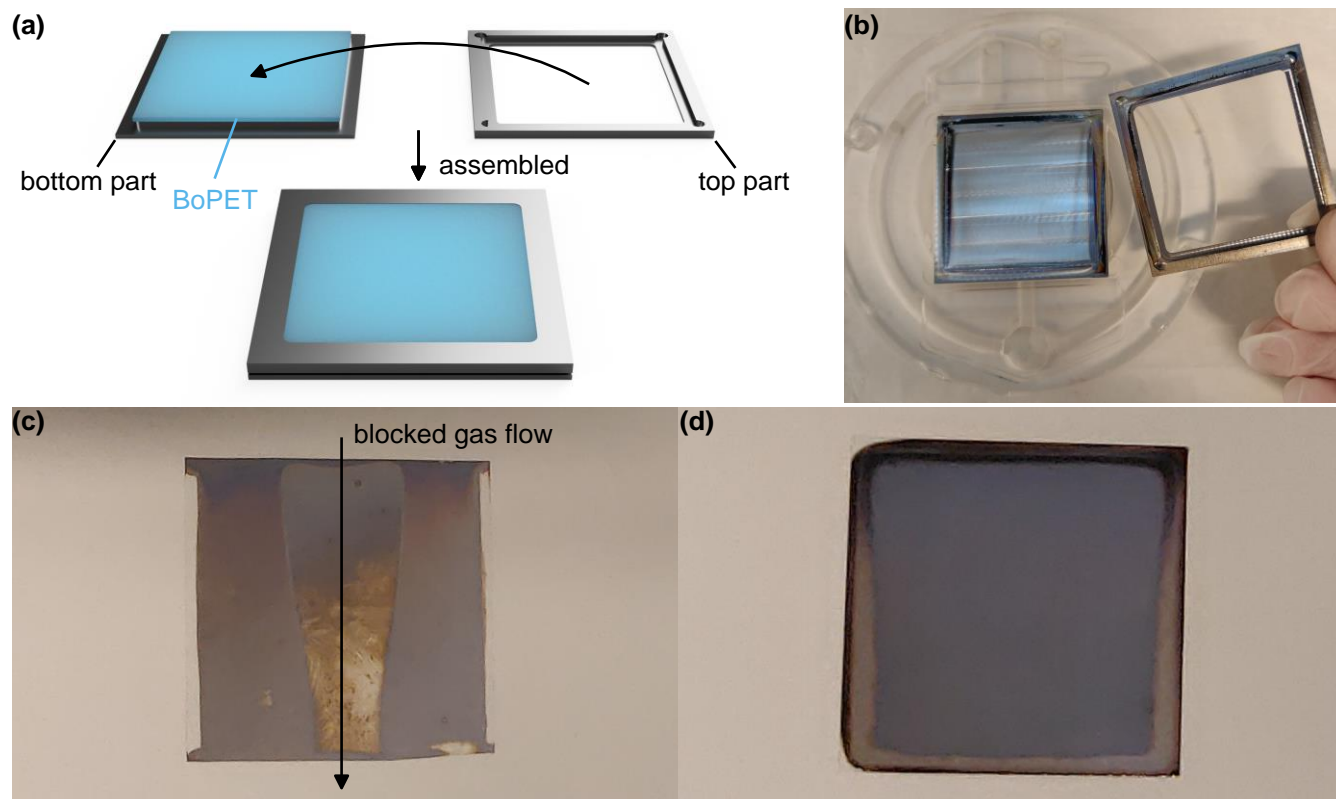


Figure S24. (a) 3D model and (b) photograph of an adapter machined from Al for depositions on BoPET. (c) BoPET after PbS deposition without using the adapter. The polymer had moved and bent inside the substrate cassette, causing a partial blockage of the gas flow. (d) BoPET after PbS deposition with the adapter.

References

- (1) Lee, S. M.; Jang, W.; Mohanty, B. C.; Yoo, J.; Jang, J. W.; Kim, D. Bin; Yi, Y.; Soon, A.; Cho, Y. S. Experimental Demonstration of in Situ Stress-Driven Optical Modulations in Flexible Semiconducting Thin Films with Enhanced Photodetecting Capability. *Chem. Mater.* **2018**, *30*, 7776–7781.
- (2) Yeon, D. H.; Lee, S. M.; Jo, Y. H.; Moon, J.; Cho, Y. S. Origin of the Enhanced Photovoltaic Characteristics of PbS Thin Film Solar Cells Processed at near Room Temperature. *J. Mater. Chem. A* **2014**, *2*, 20112–20117.
- (3) Kaci, S.; Keffous, A.; Hakoum, S.; Trari, M.; Mansri, O.; Menari, H. Preparation of Nanostructured PbS Thin Films as Sensing Element for NO₂ Gas. *Appl. Surf. Sci.* **2014**, *305*, 740–746.
- (4) Sadovnikov, S. I.; Gusev, A. I. Structure and Properties of PbS Films. *J. Alloys Compd.* **2013**, *573*, 65–75.
- (5) Kotadiya, N. B.; Kothari, A. J.; Tiwari, D.; Chaudhuri, T. K. Photoconducting Nanocrystalline Lead Sulphide Thin Films Obtained by Chemical Bath Deposition. *Appl. Phys. A Mater. Sci. Process.* **2012**, *108*, 819–824.
- (6) Göde, F.; Güneri, E.; Emen, F. M.; Emir Kafadar, V.; Ünlü, S. Synthesis, Structural, Optical, Electrical and Thermoluminescence Properties of Chemically Deposited PbS Thin Films. *J. Lumin.* **2014**, *147*, 41–48.
- (7) Silva Filho, J. M. C. da; Ermakov, V. A.; Marques, F. C. Perovskite Thin Film Synthesised from Sputtered Lead Sulphide. *Sci. Rep.* **2018**, *8*, 1563.
- (8) Mohanty, B. C.; Bector, K.; Laha, R. Elucidating Doping Driven Microstructure Evolution and Optical Properties of Lead Sulfide Thin Films Grown from a Chemical Bath. *Appl. Surf. Sci.* **2018**, *435*, 444–451.
- (9) Hone, F. G.; Dejene, F. B. Six Complexing Agents and Their Effects on Optical, Structural, Morphological and Photoluminescence Properties of Lead Sulphide Thin Films Prepared by Chemical Route. *J. Lumin.* **2018**, *201*, 321–328.
- (10) Cheraghizade, M.; Jamali-Sheini, F.; Yousefi, R. Optical, Electrical, and Photovoltaic Properties of PbS Thin Films by Anionic and Cationic Dopants. *Appl. Phys. A Mater. Sci. Process.* **2017**, *123*, 1–9.
- (11) Veena, E.; Bangera, K. V.; Shivakumar, G. K. Effect of Annealing on the Properties of Spray-Pyrolised Lead Sulphide Thin Films for Solar Cell Application. *Appl. Phys. A* **2017**, *123*, 366.
- (12) Abbas, M. M.; Shehab, A. A.-M.; Hassan, N.-A.; Al-Samuraee, A.-K. Effect of Temperature and Deposition Time on the Optical Properties of Chemically Deposited Nanostructure PbS Thin Films. *Thin Solid Films* **2011**, *519*, 4917–4922.
- (13) Azadi Motlagh, Z.; Azim Araghi, M. E. Effect of Annealing Temperature on Optical and Electrical Properties of Lead Sulfide Thin Films. *Mater. Sci. Semicond. Process.* **2015**, *40*, 701–707.
- (14) Thangavel, S.; Ganesan, S.; Saravanan, K. Annealing Effect on Cadmium in Situ Doping of Chemical Bath Deposited PbS Thin Films. *Thin Solid Films* **2012**, *520*, 5206–5210.
- (15) González-Lúa, R.; Escorcia-García, J.; Pérez-Martínez, D.; Nair, M. T. S.; Campos, J.; Nair, P. K. Stable Performance of Chemically Deposited Antimony Sulfide-Lead Sulfide Thin Film Solar Cells under Concentrated Sunlight. *ECS J. Solid State Sci. Technol.* **2015**, *4*, Q9–Q16.
- (16) Dasgupta, N. P.; Lee, W.; Prinz, F. B. Atomic Layer Deposition of Lead Sulfide Thin Films for Quantum Confinement. *Chem. Mater.* **2009**, *21*, 3973–3978.
- (17) Cardona, M.; Greenaway, D. L. Optical Properties and Band Structure of Group IV-VI and Group V Materials. *Phys. Rev.* **1964**, *133*, A1685–A1697.